Gradient mechanism in a communication network

Satyam Mukherjee* and Neelima Gupte†
Department of Physics, Indian Institute of Technology, Madras, Chennai 600036, India
(Received 18 April 2007; revised manuscript received 7 December 2007; published 24 March 2008)

We study the efficiency of the gradient mechanism of message transfer in a two-dimensional communication network of regular nodes and randomly distributed hubs. Each hub on the network is assigned some randomly chosen capacity and hubs with lower capacities are connected to the hubs with maximum capacity. The average travel times of single messages traveling on the lattice decrease rapidly as the number of hubs increase. The functional dependence of the average travel times on the hub density shows q-exponential behavior with a power-law tail. We also study the relaxation behavior of the network when a large number of messages are created simultaneously at random locations and travel on the network toward their designated destinations. For this situation, in the absence of the gradient mechanism, the network can show congestion effects due to the formation of transport traps. We show that if hubs of high betweenness centrality are connected by the gradient mechanism, efficient decongestion can be achieved. The gradient mechanism is less prone to the formation of traps than other decongestion schemes. We also study the spatial configurations of transport traps and propose minimal strategies for their elimination.

DOI: 10.1103/PhysRevE.77.036121 PACS number(s): 89.75.Hc

I. INTRODUCTION

Transport processes on networks have been a topic of intensive research in recent years. Examples of transport processes on networks include the traffic of information packets [1–4], transport processes on biological networks [5,6], and road traffic. The structure and topology of the network, as well as the mechanism of transport, have been seen to play crucial roles in the optimization of the efficiency of the transport process [7]. It is therefore important to study this interplay in the context of realistic networks so that their performance can be optimized.

Gradient networks, i.e., networks where transport efficiencies are driven by local gradients of a scalar, have been the focus of recent studies [8–10]. Examples of this include electric current and heat flow which are driven by local gradients of potential and temperature and biological transport processes such as cell migration [11]: chemotaxis, haptotaxis, and galvanotaxis [8]. Gradient networks are also seen in computer and communication networks. In the context of packet transfer, a given computer or router [12] usually asks its neighbors on the network for their current packet load and balances its load with the neighbor that has the minimum number of packets to route. In this case, the scalar is the negative of the number of packets that are routed and a directed flow is induced along the gradient of the scalar. The gradient strategy is considered to be particularly efficient in the case of simultaneous transfer of multiple messages, when congestion effects can occur on the lattice. However, the efficiency of transport of the gradient strategy depends crucially on the topology of the underlying substrate network. A gradient based on a random graph topology tends to get easily congested, in the large network limit, whereas if the substrate network is scale-free [13], then the corresponding gradient network is the least prone to congestion [8]. A congestion driven gradient, as in the router case, has also been studied [10].

In this paper, we study the efficiency of the message transport by the gradient mechanism on a two-dimensional substrate communication network of nodes and hubs. Models based on two-dimensional lattices have been studied earlier in the context of navigation and search algorithms [14] and communication networks of hosts and routers [15–17]. We study the efficiency of a gradient based on this network both for single message transfer as well as for the simultaneous transfer of multiple messages [18,19]. We also compare the efficiency of the gradient mechanism with other strategies like random assortative connections between hubs which have been considered for this network.

The connectivity of the network is determined by the nature of the two types of nodes: The regular or ordinary nodes which are connected to each of their nearest neighbors and the hubs which are connected to all the nodes in a given area of influence and are randomly distributed in the lattice. Thus the network incorporates local clustering and geographical separations [20,21]. The hubs in the lattice form a random geometry, similar to that of random geometric graphs [22], whereas the ordinary nodes have a regular geometry.

In the absence of the hubs each node has the same degree of connectivity and the degree distribution is a δ function with a single peak at four, the number of nearest neighbors; however, due to the presence of hubs the degree distribution is bimodal [23]. Thus the degree distribution of this network does not belong to the usual classes, namely, the small world [24] or scale free classes of networks, or to that of random graphs [13].

The gradient mechanism of message transfer is implemented on this substrate lattice by distributing the hubs randomly on the lattice and choosing the message handling capacities of the hubs out of a random distribution. Connections between hubs are made by the gradient mechanism where the gradient is along the steepest ascent for the capacities associated with the hubs. The connections between

*mukherjee@physics.iitm.ac.in
†gupte@physics.iitm.ac.in

hubs provide short pathways on the lattice, thereby speeding message transfer. In the absence of the gradient connections, the average travel time for messages traveling between the source and target on the base network plotted as a function of hub density showed stretched exponential behavior [23]. If the gradient mechanism is implemented on the lattice, the average travel time for single messages, traveling between source and target pairs separated by a fixed distance, shows q-exponential behavior as a function of hub density. Similar q-exponential behavior is observed if the hubs are connected by random assortative connections, i.e., each hub is connected to two or three randomly chosen other hubs. The tails of the q-exponential distribution in both cases show power-law behavior. This is consistent with the power-law behavior observed earlier at high hub densities for the random assortative connections [23]. Thus average travel times reduce very rapidly with hub densities in this regime. The origin of the q exponential may lie in the fact that our travel times are highly correlated due to many paths traveling through common hubs.

The distribution of travel times of single messages for the gradient connections shows log-normal behavior similar to that seen in the distribution of latency times of the internet [16] and in directed traffic networks [25]. The leading behavior of the travel time distribution is also log-normal when the hubs are connected by random assortative connections, but develops an additive power-law correction. In contrast, it is interesting to note that travel-time distributions for stationary traffic flow for the Webgraph shows power-law behavior, whereas the Statnet shows q-exponential behavior [26]. It was observed that the cumulative probability distribution of sparseness time intervals in the internet shows q-exponential behavior [27].

In real networks such as telephone, traffic, and computer networks, as well as the Internet, congestion effects occur under multiple message transfer due to limitations of capacity, bandwidth, and network topology [28–32]. Strategies to decongest networks [33–37] are hence of practical importance. Since the gradient scheme has proved to be quite efficient at relieving congestion in scale free networks [10], we test the efficacy of the gradient scheme for decongestion of our two-dimensional substrate network. Here, a gradient is set up between hubs of high coefficients of betweenness centrality (CBC) [34] and its success is compared with other assortative schemes.

The existence of transport traps has been observed to play a crucial role in congesting transport on scale-free networks [10,38]. Since our network incorporates geographical information, we study the spatial configuration of traps, the reasons for their formation, and their contribution to the congestion process. We also propose minimal strategies for the decongestion of traps.

The two-dimensional (2D) substrate model and the gradient mechanism for message transfer is discussed in Sec. II. We also discuss travel time distributions and their finite size scaling for single message travels in this section. In Sec. III we study multiple message transfer and the congestion problem and the efficiency of a CBC driven gradient for decongesting the network. In Sec. IV, we study the spatial distribution of trapping configurations and their contribution to congestion. We also propose strategies for the elimination of traps. In each section, we compare the behavior of the gradient mechanism with that of other assortative mechanisms. We conclude in the final section.

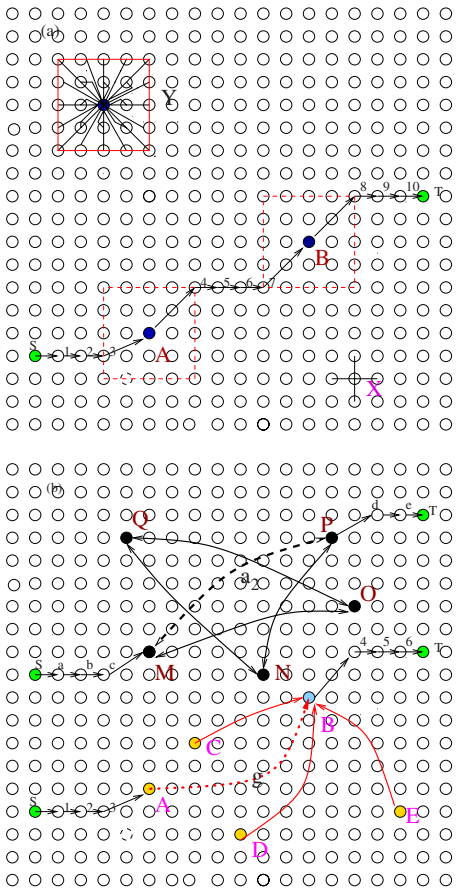

FIG. 1. (Color online) (a) Two-dimensional lattice of 20×20 nodes. X is an ordinary node with nearest neighbor connections. Each hub has a square influence region (as shown for the hub Y). A typical path from the source S to the target T is shown with labeled sites. The path S-1-2-3-A-4-5-6-7-B-8-9-10-T passes through the hubs A and B. (b) Hubs $A-E$ are distributed randomly in the lattice and each hub is assigned with some message capacity between 1 and 10. In the figure B has maximum capacity 10. The hubs are connected by the gradient mechanism as shown by one-way arrows. After the implementation of the gradient mechanism the distance between A and B is covered in one step. The gradient path is given by S-1-2-3-g-8-9-10-T. Hubs $M-Q$ are connected by two-way assortative linkages with two connections per hub. A typical path from S to T after the implementation of the two-way assortative mechanism between the hubs is shown by S -a-b-c-M-$\mathbf{a_2}$-P-d-e-T.

II. GRADIENT MECHANISM OF MESSAGE TRANSFER

The substrate model on which message communication takes place is shown in Fig. 1(a). This is a regular two-dimensional lattice with two types of nodes: The regular nodes, connected to their nearest neighbors [e.g., node X in Fig. 1(a)], and hubs at randomly selected locations which are connected to all nodes in their area of influence, a square of

side a (e.g., node Y in the same figure). We set free boundary conditions. If a message is routed from a source S to a target T on this lattice through the baseline mechanism, it takes the path S-1-2-3-A-4-5-6-7-B-8-9-10-T as in Fig. 1(a).

To set up the gradient mechanism, we need to assign a capacity to each hub, the hub capacity being defined to be the number of messages the hub can process simultaneously. Here, each hub is randomly assigned some message capacity between one and $C_{\max}$. A gradient flow is assigned from each hub to all the hubs with the maximum capacity ($C_{\max}$). Thus the hubs with lower capacities are connected to the hubs with highest capacity $C_{\max}$ by the gradient mechanism. In Fig. 1(b) if hub A has capacity 5 and hub B has capacity 10, then a flow can occur from A to B as shown by the dotted line g. Thus the hubs with the highest capacity $C_{\max}$ are maximally connected by the gradient mechanism. After the implementation of the gradient mechanism, the distance between A and B is covered in one step as shown by the link g and a message is routed along the path S-1-2-3-A-g-B-4-5-6-T as shown in Fig. 1(b). Note that gradient mechanism is essentially a one way mechanism (as shown by g). The same figure, Fig. 1(b), also shows the assortative mechanism considered earlier for transport on this network [23]. Here, each hub is connected assortatively to two other hubs randomly chosen from the other hubs. In the assortative scheme a message is routed along the path S-a-b-c-M-$\mathbf{a_2}$-P-d-e-T. The assortative mechanism, unlike the gradient mechanism, can be one way or two way. We will compare the efficiency of these two schemes for single message and multiple messages transport in later sections of this paper.

A. Routing protocol

The following routing protocol is followed by messages which travel on the lattice above. Consider a message that starts from the source S and travels toward a target T. Any node which holds the message at a given time (the current message holder), transfers the message to the node nearest to it, in the direction which minimizes the distance between the current message holder and the target. If a constituent node is the current message holder, it sends the message directly to its own hub. When the hub becomes the current message holder, the message is sent to the constituent node within the square region, the choice of the constituent node being made by minimizing the distance to the target. When a hub in the lattice becomes the current message holder, the message is transferred to the hub connected to the current message holder by the gradient mechanism, if the new hub is in the direction of the target, otherwise it is transferred to the constituent nodes of the current hub. The constituent node is chosen such that the distance from target is minimized. If there is degeneracy, i.e., there exists simultaneously more than one gradient path, we choose the one nearest to the target. When a message arrives at its target it is removed from the network. If a message reaches the boundary of the network it remains at the boundary.

Two nodes with coordinates (is,js) and (it,jt) separated by a fixed distance $D_{st}=|is-it|+|js-jt|$ are chosen from a lattice of a given size L^2, and assigned to be the source and target. The average travel time for a message for a fixed source-target distance is a good measure of the efficiency of the network. In our simulations, the travel time is calculated for a source-target separation of $D_{\rm st}=142$ on a 100×100 lattice, and averaged over 50 hub realizations and 1000 source-target pairs, with $C_{\max}=10$ and $a=3$. These values of $C_{\max}$ and a are retained for all simulations in this paper.

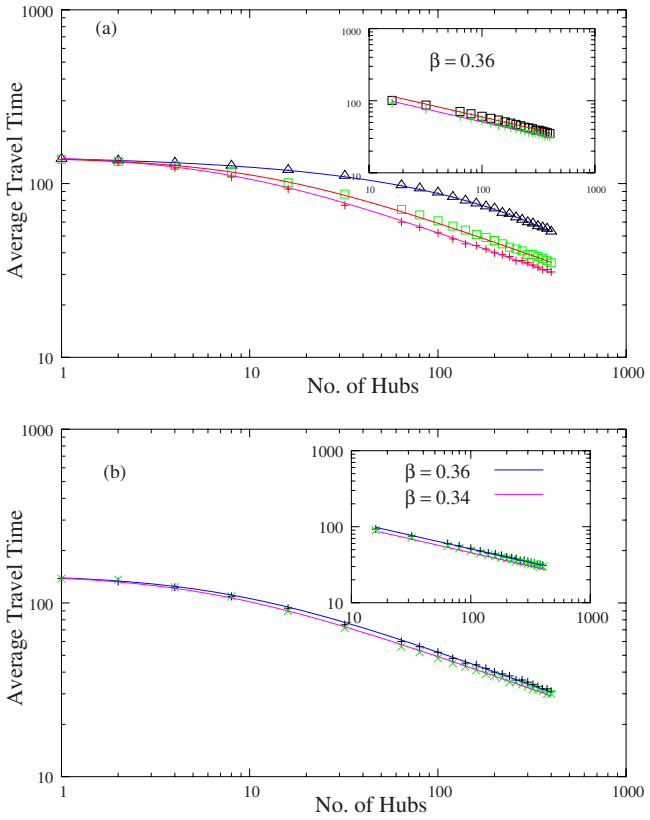

FIG. 2. (Color online) (a) Average travel time as a function of hub density follows a stretched exponential behavior (Δ) when the hubs are not connected. If the hubs are connected by gradient as well as one-way assortative mechanism, it follows a q-exponential behavior. Here $q=3.51$ for the gradient mechanism ($\square$) as well as the one-way assortative mechanism (+). (b) Here $q=3.51$ for the one-way mechanism (+) and $q=3.58$ for the two-way assortative mechanism ($\times$). As observed, when the hubs are connected by the assortative mechanisms or by the gradient mechanism, the tail of the travel time as function of hub density follows a power law behavior with similar power law exponents. In (a) (inset) for both the gradient mechanism and the one-way assortative mechanism $\beta=0.36$. In (b) (inset) $\beta=0.34$ for the two-way assortative mechanism.

B. Travel time distributions and finite size scaling

The behavior of average travel time as a function of the number of hubs for a fixed distance $D_{\rm st}$ between the source-target pairs is plotted in Fig. 2 for a 100×100 lattice and $D_{\rm st}$ of 142. The plot shows data for the original network, as well for the gradient scheme applied in the network. The stretched exponential function $f(x)=Q\exp[-Ax^{\alpha}]$, where the constants take the values $\alpha=0.50\pm0.01$, $A=0.05$, and $Q=146$, gives

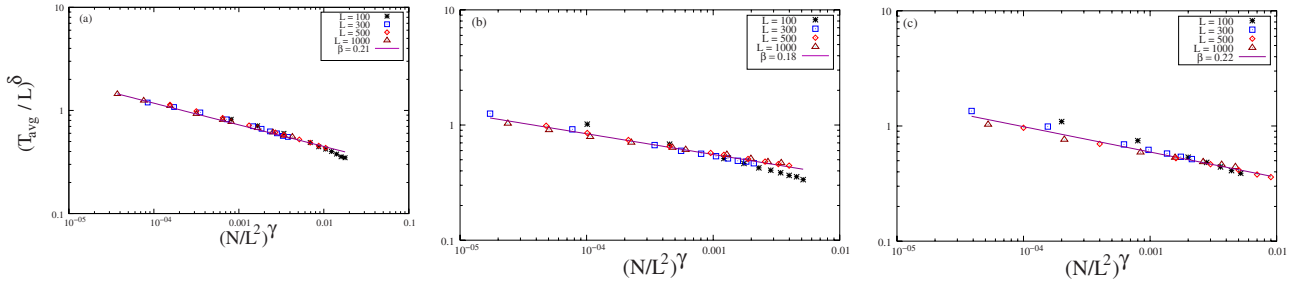

FIG. 3. (Color online) Data for $L \times L$ two-dimensional lattices for different values of L are seen to collapse on top of each other. It is seen that the final curve fits a power law of the form $Ax^{-\beta}$. (a) $A=0.17$ and $\beta=0.21\pm0.002$ for the gradient mechanism. (b) $A=0.16$ and $\beta=0.18\pm0.02$ for the two-way assortative mechanism. (c) $A=0.13$ and $\beta=0.22\pm0.002$ for the one-way assortative mechanism.

an excellent fit to the data on the original network. However, the gradient data are fitted best by the function $f(x)=A[1-(1-q)x/x_0]^{1/(1-q)}$ with the parameters $q=3.51$, $A=142$, and $1/x_0=0.03$. Thus the average travel time as a function of the number of hubs shows q-exponential behavior [39].

We plot the data for average travel times for one-way assortative connections in Fig. 2. The data can be fitted very well by a q-exponential function with the parameters $q=3.51$. When the number of hubs exceeds 10, the tail of the distribution can be fitted very well by a power law $a(x)=P_a x^{-\beta}$, where $\beta=0.34\pm0.002$ and $P_a=230$ [see inset of Fig. 2(a)], in agreement with the earlier results. The same inset shows the tail of the travel time distribution for the gradient case. It is clear that this also fits a power-law $g(x)=P_g x^{-\beta}$, where $\beta=0.36\pm0.006$ and $P_g=310$. Thus travel times for both the gradient and the one-way assortative connections show q-exponential behavior with tails which can be approximated by power laws. The values of the q exponents as well as the values of the exponent β of the gradient and the one-way case agree very well. We plot the data for average travel times as a function of number of hubs for both one-way and two-way assortative connections in Fig. 2(b). It is clear that both one-way and two-way connections show q-exponential behavior with power law tails, but the exponents differ slightly as can be seen from the values in the captions. Thus the results for the random assortative connections are in agreement with earlier observations when power-law behavior was seen for high hub densities [23]. Earlier studies of networks with growing rules which incorporate memory effects have shown q-exponential behavior in the degree distributions [40,41]. It is interesting to note that both the gradient network and the assortative connections show a q-exponential distribution in the travel times. The origin of this behavior may lie in the long range connections between the hubs which effectively reduces the distances in the system compared to its linear size. We also note that the q-exponential does not fit the baseline data for this quantity.

The dependence of the average travel times as a function of hub density discussed above was studied for a 100×100 lattice with a D_{st} value of 142. However, our results are independent of lattice size. We consider this dependence for lattices of side $L=300$, 500, and 1000 and corresponding D_{st} values of 424, 712, and 1420, respectively. We consider both the gradient case and the case where the connections are assortative.

Finite size scaling is observed if we plot $(T_{avg}/L)^{\delta}$ against $(N/L^2)^{\gamma}$ for different lattice size L (Fig. 3). Figure 3(a) plots this behavior for the gradient mechanism. It is seen that the data observed for different lattice sides L collapse onto each other for the choice $\delta=1$ and $\gamma=1.03$. The corresponding data for the assortative mechanism is shown in Fig. 3(b). Here the data collapse is observed for $\delta=0.88$ and $\gamma=1.05$ for the two-way assortative mechanism and $\delta=1$ and $\gamma=1$ for the one-way assortative mechanism. Thus the scaling law is

$$T_{avg} = L^{\mu} f\left(\frac{N}{L^2}\right)^{\gamma/\delta}. \tag{1}$$

It is seen that the data for the gradient mechanism scales as a good power law up to the scale $(N/L^2)^{\gamma}=0.001$. The power law fit for the assortative mechanism is not as good as that for the gradient mechanism but scales over a longer stretch with the cutoff Fig. 3(b) at $(N/L^2)^{\gamma}=0.005$.

The distribution of travel times for messages traveling in the lattice also shows finite size scaling. We considered lattices with sides $L=100$, 300, 500, and 1000, respectively. The hub density is taken to be 0.5% for all the above cases.

The distribution of travel times turns out to have the scaling form

$$P(t) = \frac{1}{t_{max}} G\left(\frac{t}{t_{max}}\right), \tag{2}$$

where t_{max} is the value of t at which $P(t)$ is maximum. In a similar context, it was observed that distribution of optimal path lengths in random graphs with random weights associated with each link has a universal form [42], but no analytic expression for the universal form was specified. The data obtained for the gradient [Fig. 4(a)] can be fitted very well by a log-normal distribution [25] of the form

$$G(x) = \frac{1}{x\sigma\sqrt{2\pi}} \exp\left(-\frac{(\ln x-\mu)^2}{2\sigma^2}\right), \tag{3}$$

with $\mu=-1.44$ and $\sigma=1.47$. The data obtained for the assortative mechanisms shows longer tails than the gradient data and therefore turns out to conform to a log-normal function with a power law correction of the form

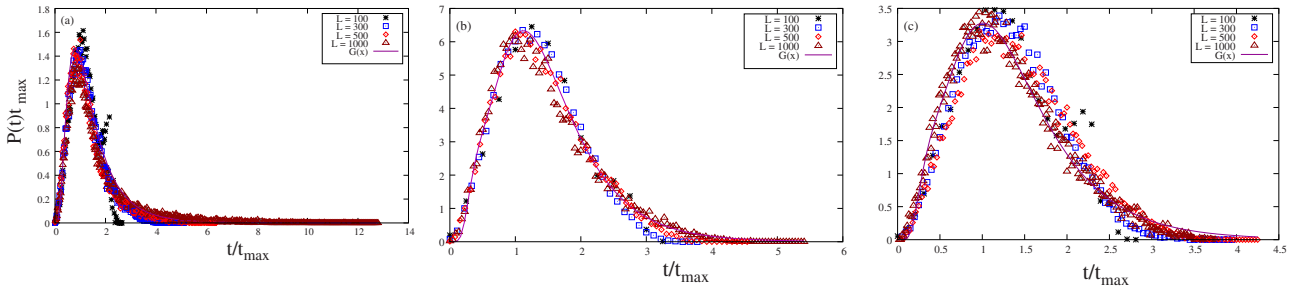

FIG. 4. (Color online) Scaled travel time distribution for (a) the gradient mechanism, (b) the two-way assortative mechanism, and (c) the one-way assortative mechanism. Different symbols represent lattices of different sizes. (a) The data are fitted by a log-normal distribution [Eq. (3)], where $\mu=-1.44$ and $\sigma=1.47$. The data for (b) and (c) are fitted by a log-normal function with a power law correction [Eq. (4)]: (b) $\mu=-0.08$, $\sigma=1.04$, and $\beta=4.51\pm0.20$; (c) $\mu=-0.33$, $\sigma=1.08$, and $\beta=4.25\pm0.12$.

$$G(x)=\frac{1}{x\sigma\sqrt{2\pi}}\exp\left(-\frac{(\ln x-\mu)^2}{2\sigma^2}\right)(1+Bx^{-\beta}), \qquad (4)$$

where $\mu=-0.08$, $\sigma=1.04$, and $\beta=4.51\pm0.20$ for the two-way assortative mechanism [Fig. 4(b)] and $\mu=-0.33$, $\sigma=1.08$, and $\beta=4.25\pm0.12$ for the one-way assortative mechanism [Fig. 4(c)]. Similar log-normal behavior is obtained for latencies in the internet [16] and in the directed traffic flow [25]. Similar finite size scaling is observed from hub densities above 0.1%. Below this value, we see a bimodal distribution in the travel times due to the contribution of the nodes and the hubs [23], and no finite size scaling is observed.

III. CONGESTION AND DECONGESTION

In the previous section, we studied average travel times, and travel time distributions, for single messages traveling on the network. In this section, we consider a large number of messages which are created at the same time and travel toward their destinations simultaneously. The hubs on the lattice, and the manner in which they are connected, are the crucial elements which control the subsequent relaxation dynamics, and hence influence the "susceptibility" of the network. On the one hand, it is clear that the hubs provide short paths through the lattice. On the other hand, when many messages travel simultaneously on the network, the finite capacity of the hubs can lead to the trapping of messages in their neighborhoods, and a consequent congestion or jamming of the network. A crucial quantity which identifies these hubs is called the coefficient of betweenness centrality (CBC) [34], defined to be the ratio of the number of messages N_k which pass through a given hub k to the total number of messages N which run simultaneously, i.e., CBC $=N_k/N$. Hubs with higher CBCs are more prone to congestion. We compare the efficiency of the gradient mechanism with one-way and two-way assortative CBC mechanisms. We study our network in the congested phase where messages are trapped at such hubs, examine the spatial configurations of the traps, and the success of decongestion strategies.

The gradient mechanism studied here is set up as follows. We choose η top ranking hubs ranked according to their CBC values. In the CBC driven gradient mechanism we enhance the hub capacities of the η hubs, proportional to their CBC values by a factor of κ. The fractional values are set to the nearest integer values. The hubs are connected by the gradient mechanism.

We choose N source-target pairs randomly, separated by a fixed distance D_{st} on the lattice. All sources send messages simultaneously to their respective targets at an initial time $t=0$. The messages are transmitted by a routing mechanism similar to that for single messages, except when the next node or hub on the route is occupied. We carry out parallel updates of nodes.

If the would be recipient node is occupied, then the message waits for a unit time step at the current message holder. If the desired node is still occupied after the waiting time is over, the current node selects any unoccupied node from its remaining neighbors and hands over the message. If all the neighboring nodes are occupied, the message waits at the current node until one of them is free. If the current message holder is the constituent node of a hub (the temporary target [34]) which is occupied, the message waits at the constituent node until the hub is free. The rest of the routing is as described in Sec. II for single messages.

In our simulation we choose $\eta=5$ and $\kappa=10$. We choose a network of (100×100) nodes with $N=2000$ messages and $D_{st}=142$. It is to be noted that just five hubs on the lattice have extra connections in this case, unlike the previous section where every hub has two extra connections. The fraction of messages delivered at the end of the run for given hub density is shown in Table I. It is clear that the gradient mechanism shows a substantial improvement over the baseline.

Other decongestion mechanisms which involve hubs of high CBC have been proposed earlier. It had been observed that introducing assortative connections between hubs of high CBC has the effect of relieving congestion [34]. This is achieved in two ways: (i) One-way (CBC_a) and two-way connections (CBC_c) between the top five hubs ranked by CBC; (ii) one-way (CBC_b) and two-way assortative connections (CBC_d) between each of the top five hubs and any other hub randomly chosen in the lattice. In our simulations, the capacity of the top five hubs is enhanced to five, so that these schemes are variants of the CBC scheme. We note that more than one connection per hub is possible for each one of the two cases.

TABLE I. The table shows F the fraction of messages delivered during a run time of $4D_{st}$, as a function of hub density D. The second column shows F for the baseline (lattice with unit hub capacity). The third column shows F for the CBC (lattice with augmented top five hubs). The remaining columns show the fraction of messages delivered for the gradient mechanism and assortative linkages as described in the text. The numbers in parentheses indicate the standard deviation for fraction of messages. The averaging is done over 200 hub configurations.

D	F_{base}	F_{CBC}	F_{grad}	F_{CBC_a}	F_{CBC_b}	F_{CBC_c}	F_{CBC_d}
0.5	0.156(0.04)	0.2095(0.05)	0.4695(0.08)	0.453(0.07)	0.458(0.08)	0.637(0.08)	0.647(0.08)
1.0	0.286(0.05)	0.405(0.05)	0.6185(0.07)	0.588(0.08)	0.567(0.07)	0.7195(0.07)	0.8285(0.07)
2.0	0.3755(0.06)	0.553(0.07)	0.756(0.08)	0.717(0.08)	0.749(0.04)	0.858(0.04)	0.9205(0.06)
3.0	0.723(0.08)	0.752(0.08)	0.9685(0.03)	0.938(0.04)	0.9395(0.04)	0.9425(0.03)	0.9685(0.03)
4.0	0.903(0.07)	0.868(0.07)	1.0	1.0	1.0	1.0	1.0

It is clear that the gradient, which is an inherently one-way mechanism, works better than one-way assortative connections of both kinds, viz. connections between the top five hubs themselves and the top five hubs and randomly chosen other hubs. However, it is clear from Table I that the two-way connections perform better than the gradient at some hub densities. Thus the gradient is the mechanism of choice in any setup where one-way connections are optimal.

The same conclusions can be drawn from Fig. 5, which shows the plot $N(t)$, the number of messages running in the lattice at time t, as a function of t for each of these cases, again with the parameters $\eta=5$ and $\kappa=10$, on a network of (100×100) nodes with $N=2000$ messages, $D_{st}=142$ and a run time of 5000 time steps. Figure 5(a) is plotted for a hub density of 0.5%, and Fig. 5(b) is plotted for a hub density of 4.0%. It is clear that all messages get cleared at the higher hub density, whereas some messages remain undelivered even after 5000 time steps at the lower hub density. The number of messages remains constant, indicating that a small fraction of messages have been trapped. It is also interesting to note that the gradient mechanism is less prone to traps. As a result, there is a time at which the gradient mechanism overtakes the two-way assortative mechanisms in the delivery of messages. The spatial configuration of traps is interesting. We study this in the next section.

IV. TRAPPING CONFIGURATIONS

A detailed analysis of the transport mechanism reveals that the main cause of nondelivery of messages is the phenomenon of the formation of traps or congestion nuclei [10,43]. In the decongestion mechanisms discussed above, we studied the transport of 2000 messages. The critical value of the number of messages for which trapping occurs under various decongestion strategies is well below 2000. For high hub densities (400 hubs in 100×100 lattice), all the messages get cleared when we introduce different schemes of decongestion. Now we consider 50 hubs in a 100×100 lattice and a run time of 5000. Figure 5(a) shows that despite different decongestion mechanisms, the value of $N(t)$ saturates after a certain saturation time t_s indicating the formation of transport traps in the 2D network. These traps are formed due to various reasons like the low capacity of high CBC hubs, the opposing movement of messages from sources and targets situated on different sides of the lattice, as well as due to edge effects. As mentioned earlier, our network incorporates local clustering and geographical separations. These features have special bearing on spatial configurations of traps. In this section, we look at the spatial configuration of traps under the various assortative mechanisms.

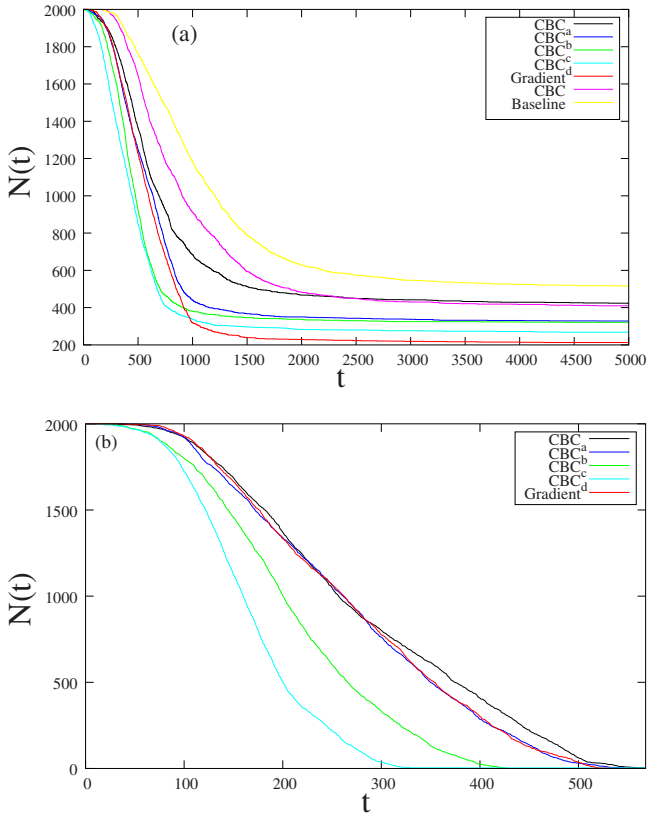

FIG. 5. (Color online) Decongestion by different mechanisms for (a) 50 hubs and (b) 400 hubs in a 100×100 lattice with $D_{st}=142$. In (a) run time is set at 5000 time steps. It is observed that after a saturation time t_s, the number of messages undelivered, $N(t)$, gets saturated, indicating the formation of transport traps in the lattice. In (b) all the messages get delivered for the assortative and gradient scheme. The run time is set at $4D_{st}$.

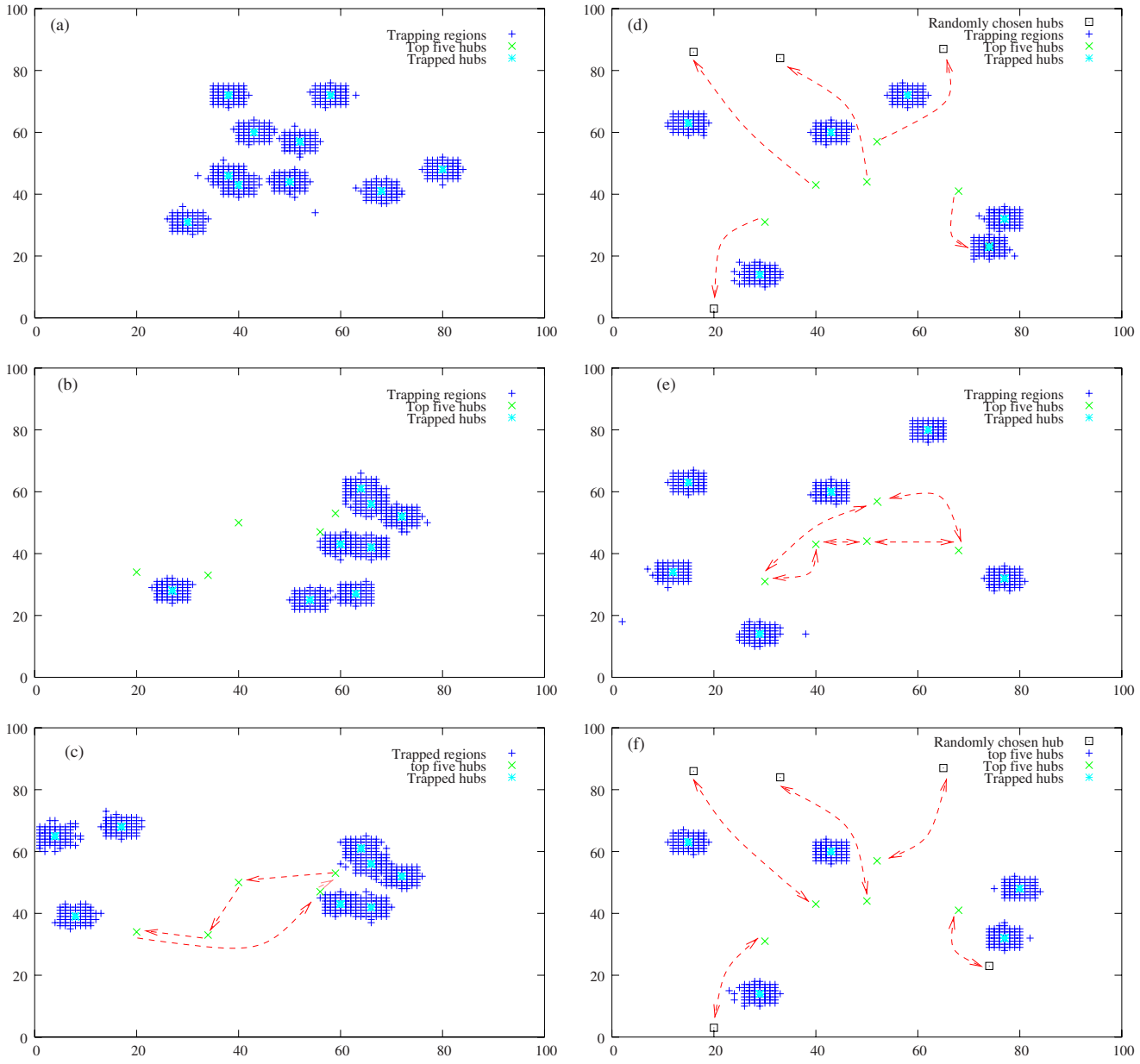

FIG. 6. (Color online) This figure shows the spatial configuration of traps. The shaded regions (+) are the trapping regions where the trapped hubs are indicated by (∗).The crosses (×) are the top five hubs. The connection between hubs are indicated by one-way and two-way dashed arrows. The figure shows trapping regions in (a) the baseline mechanism and (b) the CBC mechanism. The top five hubs (×) have enhanced capacity of value 5. (c) The CBC_a mechanism. The top five hubs (×) with enhanced capacity and connected by one-way assortative mechanism. (d) The CBC_b mechanism. Each of the top five hubs (×) with enhanced capacity has a one-way connection with any other hub chosen randomly (□) in the lattice. (e) The CBC_c mechanism. The top five hubs (×) with enhanced capacity are connected by two-way assortative mechanism. (f) The CBC_d mechanism. Each of the top five hubs (×) with enhanced capacity has a two-way connection with any other hub chosen randomly (□) in the lattice.

A. Transport traps for CBC assortative schemes

We study the spatial configuration of traps formed due to various CBC assortative schemes. In the baseline mechanism due to unit hub capacity all the top five hubs are trapped [Fig. 6(a)] and more than 25% of the messages are trapped overall (Table II). If the capacities of the top five hubs are augmented to five [Fig. 6(b), CBC in Table II], these hubs get decongested, but the traps shift to other hubs, and the number of trapped messages is still large. One-way connections between these augmented top five hubs [CBC_a, Fig. 6(c)] clear the messages faster and shift the trapped hubs to different locations, but the number of trapped messages is not reduced. One-way connections between the augmented top five hubs and randomly chosen other hubs [CBC_b, Fig. 6(e)] shift the trapped hubs and also reduce the number of trapped messages quite significantly. Two-way connections

TABLE II. The table shows the number of hubs trapped and total number of messages trapped in the lattice when different schemes for message transfer are applied. The number of messages trapped in a hub is $(2a+1)^2$. Hence the total number of messages trapped in the hubs is $k_1(2a+1)^2$, where k_1 is the number of trapped hubs. A few messages, say n_1, get trapped in the ordinary nodes adjacent to the constituent nodes of a hub. The total number of messages trapped in the lattice after a given run time is given by $k_1(2a+1)^2+n_1$. We chose 50 hubs in 100×100 lattice and a run time of 5000. For the CBC cases only the top five hubs have capacity enhanced to 5. The numbers in parentheses indicate the standard deviation for messages. The averaging is done over 200 hub configurations.

Mechanism	No. of trapped hubs	Messages trapped	Hub capacity	Saturation time
Baseline	10	515(76)	1	2500
CBC	8	410(109)	5	2000
CBC_a	8	413(93)	5	1500
CBC_b	6	328(102)	5	1250
CBC_c	6	321(69)	5	1000
CBC_d	5	268(50)	5	1000

among the top five hubs themselves [CBC_c, Fig. 6(d)] perform at par with the CBC_b mechanism. Two-way connections among the top five hubs and randomly chosen other hubs [CBC_d, Fig. 6(f)] work the most efficiently, as can be seen from the data on the number of trapped hubs and the total number of trapped messages in Table II.

It is to be noted that no method of reconnecting the hubs eliminates all traps from the lattice. The geographical location of the traps indicates that some of the trapping is due to edge effects.

B. Transport traps in gradient schemes

We now examine the trapping configurations in different gradient schemes. We have discussed the single star gradient mechanism in Fig. 1(b), where the star was formed by applying the gradient to the top five hubs ranked by CBC. It is clear that the topology of the single star gradient configuration is different from that of the assortative connections between the top five hubs [Fig. 1(b)]. Moreover, the capacities of the top five hubs are different when connected by the gradient scheme, unlike in the CBC assortative schemes, where the capacities of all the top five hubs are enhanced equally. It was observed earlier that the star configuration provides optimum transport in a network [29,44]. We also found that, for a long run time (5000 steps), this mechanism clears a larger number of messages than other decongestion mechanisms discussed above [Fig. 5(a)]. However, a few messages still remain trapped in this scheme [Fig. 5(a), Table III]. We try the double star gradient to achieve detrapping here. In the double star gradient mechanism we form the first star by applying the gradient mechanism to the top five hubs ranked by CBC, and the second star by applying the gradient to the next top five hubs. We also connect the double star by applying one-way and two-way connections between the central hubs as shown in Fig. 7.

TABLE III. The table shows the number of hubs trapped and total number of messages trapped in the lattice when different CBC driven gradient schemes for message transfer are applied. We chose 50 hubs in 100×100 lattice and a run time of 5000. The position of the central hub for single star configuration is (50,44) and that for double star configuration is (50,44) and (29,14). (DS)* indicates double star with augmented central hubs. The numbers in parentheses indicate the standard deviation for messages. The averaging is done over 200 hub configurations.

Gradient mechanism	No. of trapped hubs	Messages trapped	Saturation time	Capacity of central hubs
Single star	4	213(75)	1200	10
Double star (DS)	3	157(39)	1400	10,4
(DS) one way	6	308(120)	1800	10,4
(DS) two way	4	205(73)	1250	10,4
(DS)*	1	54(16)	1200	20,8
(DS)* one way	0	0	-	20,8
(DS)* two way	0	0	-	20,8

Figure 9 shows the trapping regions in the double star configuration. The double star configuration [Fig. 9(b)] clears messages faster than the single star configuration [Fig. 9(a)] due to the presence of additional short cuts. If the capacity of the central hub of the double star is doubled, some

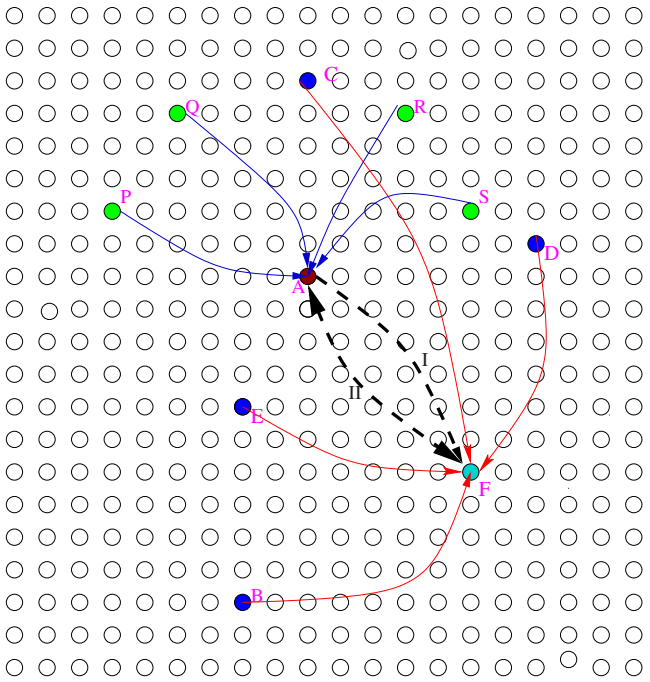

FIG. 7. (Color online) Double star configuration. The hubs B, C, D, E, F are the top five hubs and A, P, Q, R, S are the next in order of CBC. The hubs A and F are the central hubs for their respective star configurations. The dotted line I is a one-way connection between A and F. The dotted line II represents a two-way connection between A and F.

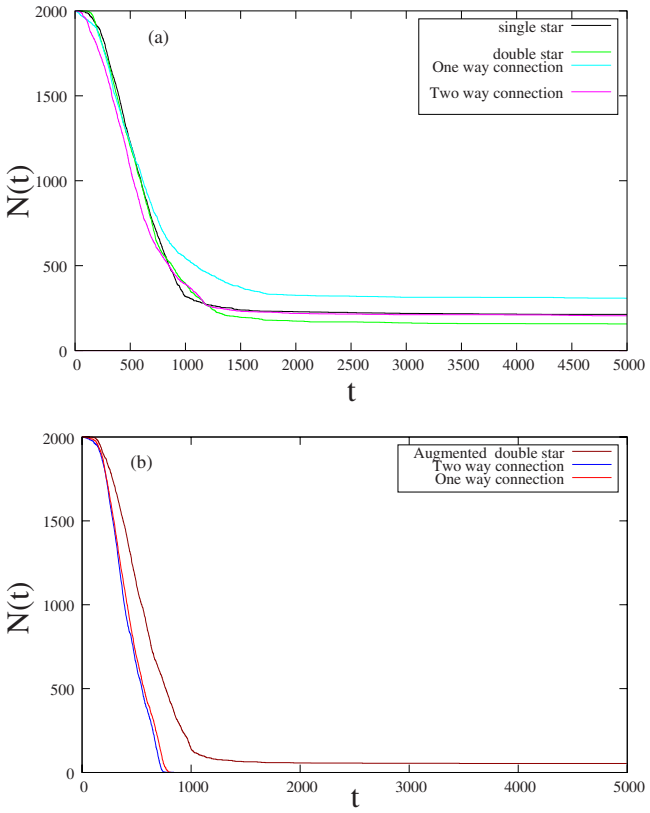

FIG. 8. (Color online) (a) Trapping in different types of gradient schemes for 50 hubs in a 100×100 lattice. The run time is set at 5000. (b) Messages clear faster when the capacity of the central hubs of double star configuration are augmented. Total decongestion occurs when we introduce one-way and two-way connections between the two central hubs of the double star and double their capacities to that of their original values. We considered 50 hubs in 100×100 lattice.

messages still remain undelivered. (See Table III as well as Fig. 8.) If one-way assortative connections [Fig. 9(c)] are added between the central hub of each star, the situation does not improve and messages get trapped in the vicinity of the central hubs. The introduction of two-way connections [Fig. 9(d)] improves the situation, but still does not clear the congestion completely. In order to clear the congestion completely, we need to enhance the capacity of the central hubs of the two stars (Table III) as well as add an assortative connection between the two central hubs. If the capacity of these two central hubs is doubled relative to their original capacity, all the messages get cleared for both the assortative one-way and two-way cases [Fig. 8(b)]. Thus the capacity of the central hubs of the stars remains the limiting factor in the clearing of congestion. However, due to the optimal nature of the double star with two connections configuration, an increase of capacity at just the two central hubs of the star is sufficient to relieve congestion. We observed that messages do not hop between any of the connected central hubs as in [10].

As seen in Tables II and III, the standard deviation for messages trapped is quite large. This is due to the large fluctuations during trapping of messages as compared to the free flow states (Table I) where messages get cleared during a run time of $4D_{\mathrm{st}}$.

C. Elimination of trapping effects

As seen above, the occurrence of transport traps is unavoidable in networks which incorporate hubs. On the other hand, the existence of hubs is essential for providing short paths and short travel times on the network. In the case of the gradient mechanism, the elimination of trapping effects in the double star configuration needed a combination of addition of connectivity, as well as capacity enhancement. This is a static strategy. Static and dynamic strategies of message routing have been considered earlier for communication networks [45]. In this section we outline two dynamic strategies of eliminating trapping effects. One involves capacity enhancement and the other involves rerouting. The new strategies are invoked after the number of messages which reach the target has saturated, that is at times which exceed t_s.

In strategy I, we enhance the capacity of the temporary targets of the trapped messages by unity. The number of messages running on the lattice at time t as a function of time can be found in Table IV. Each column is labeled by the nature of the substrate network on which the messages run. The traps clear very fast (within 200 time steps) as can be seen from the table, despite the enhancement of capacity being small. The baseline clears the slowest and the gradient the fastest.

In strategy II, we bypass the transport traps by sending the messages which will encounter traps by a different route. If the temporary target of a given message turns out to be a transport trap, the message is assigned a different temporary target. The newly assigned temporary target is chosen along the direction of the final target (Table V). This strategy is not efficient for the baseline mechanism. For this case, messages start clearing only to be trapped again after a certain time. However, this strategy acts very fast when applied to the assortative network and the gradient network. It is also observed (Tables IV and V) that the fluctuations in both these two strategies are quite large during the transition from the congested (trapped) phase to the decongested phase.

It is observed that, in terms of rate of delivery of messages, strategy I is more efficient than strategy II when applied on the baseline, the CBC, the one-way assortative mechanisms, and the gradient mechanism. Strategy II performs better than strategy I when applied on the two-way assortative mechanisms, since the number of alternate paths is larger.

V. CONCLUSION

To summarize, in this paper we have studied network traffic dynamics for single message and multiple message transport in a communication network of nodes and hubs which incorporates geographic clustering. The gradient is implemented by assigning each hub on the network some randomly chosen capacity and connecting hubs with lower capacities to the hubs with maximum capacity.

The average travel time of single messages traveling on this lattice, plotted as a function of hub density, shows

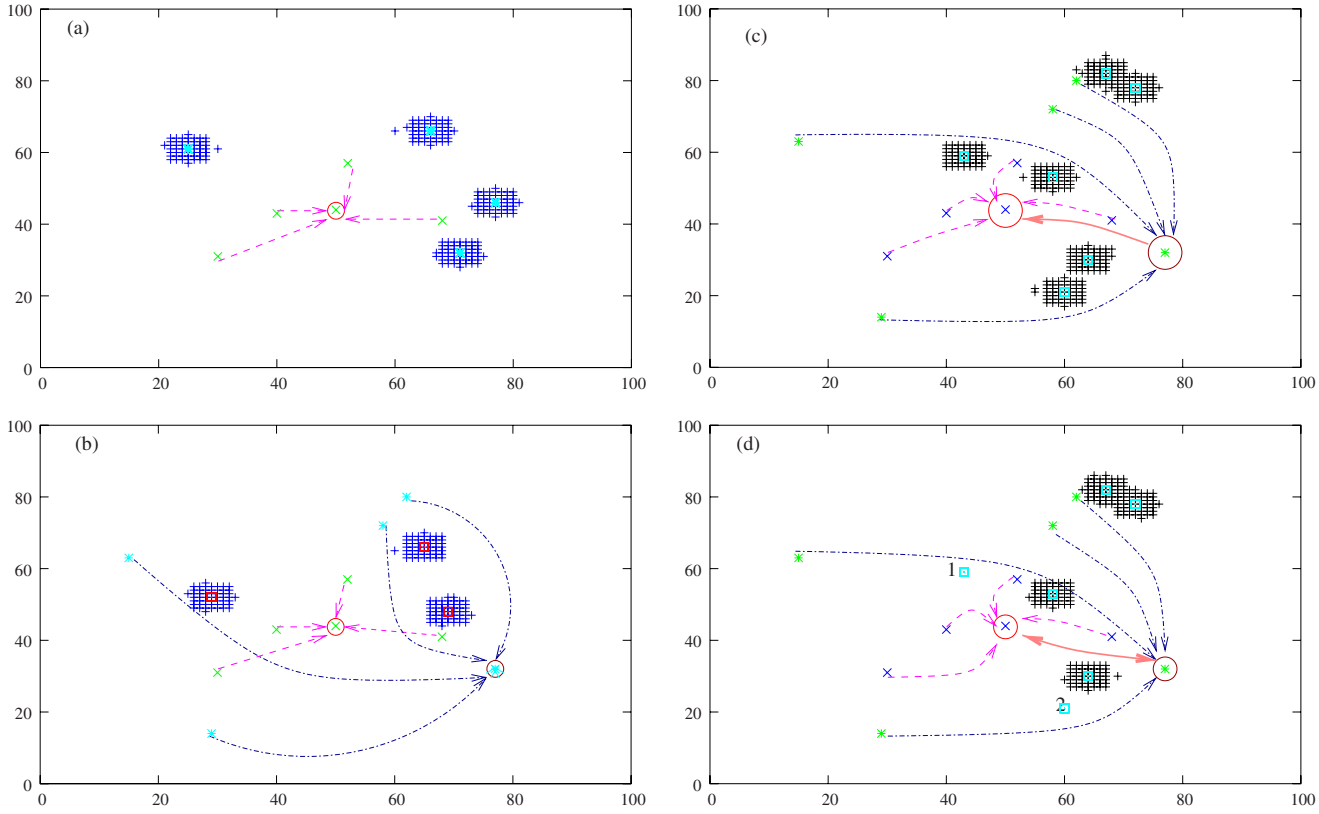

FIG. 9. (Color online) Trapping regions for 50 hubs in a 100×100 lattice in (a) the single star gradient mechanism. The capacities of the top five hubs ($\times$) are distributed proportional to their CBC values with a multiplicative factor of 10. The messages are trapped in the hubs marked by an ($*$). (b) The double star gradient mechanism. The capacities of the top five hubs ($\times$) and the next top five hubs ($*$) are distributed proportional to their CBC values with a multiplicative factor of 10. The patches (+) indicate the trapped hubs ($\square$). The number of patches are less than that for the single star configuration. (c) The one-way connection between the two central hubs ($\times$ and $*$) of the double star configuration. The shaded regions (+) are the trapping regions in the lattice, where the trapped hubs are indicated by ($\square$). (d) The two-way connection between the two central hubs ($\times$ and $*$) of double star configuration. Hubs 1 and 2 are cleared when a two-way connection between the central hubs is introduced.

stretched exponential behavior for the base network in the absence of the gradient, but shows q-exponential behavior when the hubs are connected by the gradient mechanism. This q exponential originates in the fact that our travel times are highly correlated due to many paths traveling through common hubs. The gradient between the hubs introduces short travel times on the lattice and long range correlations between the hubs. Hence the distribution of travel times for the gradient case at high hub densities shows log-normal behavior as in the case of the distribution of latencies for the internet [16] and for directed traffic flow [25]. The power law in the average travel times seen at high hub densities can be extracted from the log-normal travel time distribution at these densities [46]. However, the extraction of a q exponential from a suitable Tsallis entropy is not simple for this network. We hope to discuss this issue in future work.

Congestion effects are observed when many messages run simultaneously on the base network. However, the network decongests very rapidly when the gradient mechanism is applied to a few hubs of high coefficient of betweenness cen-

TABLE IV. The table shows the comparison of values of $N(t)$ at time t, for various decongestion schemes when strategy I is applied. The numbers in parentheses indicate the standard deviation for messages. The averaging is done over 200 hub configurations.

t	N_{base}	N_{CBC}	N_{CBC_a}	N_{CBC_b}	N_{CBC_c}	N_{CBC_d}	N_{grad}
4800	515(76)	410(113)	413(93)	328(102)	321(99)	268(89)	213(75)
4850	474(71)	329(75)	274(68)	226(70)	182(56)	151(40)	155(46)
4900	184(65)	59(20)	57(25)	71(26)	42(13)	20(4)	27(14)
4950	20(16)	1(0)	3(0)	2(0)	3(0)	2(0)	0
5000	1(0)	0	0	0	0	0	0

TABLE V. The table shows the comparison of values of $N(t)$ at time t, for various decongestion schemes when strategy II is applied. The numbers in parentheses indicate the standard deviation for messages. The averaging is done over 200 hub configurations.

t	N_{base}	N_{CBC}	N_{CBC_a}	N_{CBC_b}	N_{CBC_c}	N_{CBC_d}	N_{grad}
4800	515(76)	410(113)	413(93)	328(102)	321(99)	268(89)	213(75)
4850	513(86)	397(109)	398(101)	308(103)	155(72)	114(41)	172(49)
4900	450(69)	301(105)	285(95)	184(51)	24(16)	11(4)	50(17)
4950	323(66)	200(68)	189(37)	47(20)	4(2)	1(0)	1(0)
5000	247(55)	98(51)	58(30)	4(2)	2(1)	0	0
5050	209(42)	9(4)	1(0)	0	0	0	0
5100	187(38)	0	0	0	0	0	0

trality. The existence of transport traps can set a limit on the extent to which congestion is cleared at low hub density. The spatial configuration of traps is studied for both the gradient and other assortative decongestion schemes. We observe that the gradient mechanism which results in the formation of star configurations is substantially less prone to the formation of transport traps than other decongestion mechanisms. We also propose efficient strategies which eliminate the trapping effects either by rerouting or by minimal addition of capacity or connections at very few locations. We note that networks which incorporate geographic clustering and encounter congestion problems arise in many practical situations, e.g., cellular networks [47] and air traffic networks [48]. Networks where functional clusters are connected by long range connections arise in complex brain networks [49] and neural networks [50] as well. Our results may have relevance in these contexts.

ACKNOWLEDGMENTS

We wish to acknowledge the support of DST, India under the project SP/S2/HEP/10/2003. We thank A. Prabhakar for useful discussions.

[1] B. Tadic and G. Rodjers, Adv. Complex Syst. **5**, 445 (2002).
[2] B. Tadic and S. Thurner, Physica A **332**, 566 (2004).
[3] A. Arenas, A. Diaz-Guilera, and R. Guimera, Phys. Rev. Lett. **86**, 3196 (2001).
[4] M. Rosvall and K. Sneppen, Phys. Rev. Lett. **91**, 178701 (2003); M. Rosvall, P. Minnhagen, and K. Sneppen, Phys. Rev. E **71**, 066111 (2005); W.-X. Wang, B.-H. Wang, C.-Y. Yin, Y.-B. Xie, and T. Zhou, *ibid.* **73**, 026111 (2006).
[5] R. Albert and A. Barabasi, Rev. Mod. Phys. **74**, 47 (2002).
[6] M. E. J. Newman, SIAM Rev. **45**, 167 (2003).
[7] C.-M. Ghim, E. Oh, K.-I. Goh, B. Kahng, and D. Kim, Eur. Phys. J. B **38**, 193 (2004).
[8] Z. Toroczkai and K. E. Bassler, Nature (London) **428**, 716 (2004); Z. Toroczkai, B. Kozma, K. E. Bassler, N. W. Hengartner, and G. Korniss, e-print arXiv:cond-mat/0408262.
[9] K. Park, Y.-C. Lai, L. Zhao, and N. Ye, Phys. Rev. E **71**, 065105(R) (2005).
[10] B. Danila, Y. Yu, S. Earl, J. A. Marsh, Z. Toroczkai, and K. E. Bassler, Phys. Rev. E **74**, 046114 (2006).
[11] R. Nuccitelli, in *Pattern Formation: A Primer in Developmental Biology*, edited by G. M. Malacinski (MacMillan, New York, 1984), p. 23.
[12] Y. Rabani, A. Sinclair, and R. Wanka, *Proceedings of the 39th Symposium on Foundations of Computer Science (FOCS)* (IEEE Computer Society, Los Alamitos, CA, 1998), p. 694.
[13] A.-L. Barabasi, R. Albert, and H. Jeong, Physica A **272**, 173 (1999).
[14] J. Kleinberg, Nature (London) **406**, 845 (2000).
[15] T. Ohira and R. Sawatari, Phys. Rev. E **58**, 193 (1998).
[16] R. V. Sole and S. Valverde, Physica A **289**, 595 (2001); S. Valverde and R. V. Sole, *ibid.* **312**, 636 (2002).
[17] H. Fuks, A. T. Lawniczak, and S. Volkov, ACM Trans. Model. Comput. Simul. **11**, 233 (2001); H. Fuks and A. T. Lawniczak, Math. Comput. Simul. **51**, 101 (1999).
[18] L. Neubert, L. Santen, A. Schadschneider, and M. Schreckenberg, Phys. Rev. E **60**, 6480 (1999).
[19] J. M. Gordon and Q. F. Stout, *Fault Tolerant Message Routing on Large Parallel Systems* (IEEE, New York, 1988).
[20] C. P. Warren, L. M. Sander, and L. M. Sokolov, Phys. Rev. E **66**, 056105 (2002).
[21] A. F. Rozenfeld, R. Cohen, D. ben-Avraham, and S. Havlin, Phys. Rev. Lett. **89**, 218701 (2002).
[22] J. Dall and M. Christensen, Phys. Rev. E **66**, 016121 (2002).
[23] B. K. Singh and N. Gupte, Phys. Rev. E **68**, 066121 (2003).
[24] D. J. Watts and S. H. Strogatz, Nature (London) **393**, 440 (1998).
[25] G. Mukherjee and S. S. Manna, Phys. Rev. E **71**, 066108 (2005).
[26] B. Tadic, G. J. Rodgers, and S. Thurner, e-print arXiv:physics/0606166.
[27] S. Abe and N. Suzuki, Phys. Rev. E **67**, 016106 (2003).
[28] B. A. Huberman and R. M. Lukose, Science **277**, 535 (1997).
[29] R. Guimera, A. Diaz-Guilera, F. Vega-Redondo, A. Cabrales, and A. Arenas, Phys. Rev. Lett. **89**, 248701 (2002).
[30] Y. Moreno, R. Pastor-Sattoras, A. Vazquez, and A. Vespignani, Europhys. Lett. **62**, 292 (2003); P. Echenique, J. Gomez-

Gardenes, and Y. Moreno, Phys. Rev. E **70**, 056105 (2004).
[31] L. Zhao, Y.-C. Lai, K. Park, and N. Ye, Phys. Rev. E **71**, 026125 (2005).
[32] J. J. Wu, Z. Y. Gao, H. J. Sun, and H. J. Huang, Europhys. Lett. **74**, 560 (2006).
[33] Z. Liu, W. Ma, H. Zhang, Y. Sun, and P. M. Hui, Physica A **370**, 843 (2006); J. J. Wu, Z. Y. Gao, and H. J. Sun, Europhys. Lett. **76**, 787 (2006).
[34] B. K. Singh and N. Gupte, Phys. Rev. E **71**, 055103(R) (2005); N. Gupte and B. K. Singh, Eur. Phys. J. B **50**, 227 (2006).
[35] B. Danila, Y. Yu, J. A. Marsh, and K. E. Basler, Chaos **17**, 026102 (2007).
[36] G. Yan, T. Zhou, B. Hu, Z.-Q. Fu, and B.-H. Wang, Phys. Rev. E **73**, 046108 (2006).
[37] S. Sreenivasan, R. Cohen, E. Lopez, Z. Toroczkai, and H. E. Stanley, Phys. Rev. E **75**, 036105 (2007).
[38] L. K. Gallos, Phys. Rev. E **70**, 046116 (2004).
[39] C. Tsallis, J. Stat. Phys. **52**, 479 (1988).
[40] S. Thurner, Europhys. News **36**, 218 (2005).
[41] D. R. White, N. Kejzar, C. Tsallis, D. Farmer, and S. White, Phys. Rev. E **73**, 016119 (2006).
[42] T. Kalisky, L. A. Braunstein, S. V. Buldyrev, S. Havlin, and H. E. Stanley, Phys. Rev. E **72**, 025102(R) (2005).
[43] R. Guimera, A. Arenas, A. Diaz-Guilera, and F. Giralt, Phys. Rev. E **66**, 026704 (2002).
[44] A. Arenas, A. Cabrales, A. Diaz-Guilera, R. Guimera, and F. Vega-Redondo, Stat. Mech. Complex Netw. **625**, 175 (2003); R. Guimera, A. Diaz-Guilera, F. Vega-Redondo, A. Cabrales, and A. Arenas, Phys. Rev. Lett. **89**, 248701 (2002).
[45] D. Raghupathy, M. R. Leuze, and S. R. Schach, *Hypercube Concurrent Computers and Applications*, Proceedings of the Third Conference on Hypercube Concurrent Computers and Applications: Architecture, Software, Computer Systems, and General Issues (ACM, New York, 1988), Vol. 1.
[46] S. Mukherjee and N. Gupte, *Message Transfer in a Communication Network*, Proceedings of the Conference and Workshop "Perspectives in Nonlinear Dynamics" [Pramana (to be published)].
[47] H. Jeong, S. P. Mason, Z. N. Oltvai, and A. L. Barabasi, Nature (London) **411**, 41 (2001); H. Jeong, B. Tombor, R. Albert, Z. N. Oltvai, and A. L. Barabasi, *ibid.* **407**, 651 (2000).
[48] C. Mayer and T. Sinai, Am. Econ. Rev. **93**, 4 (2003).
[49] C. Zhou, L. Zemanova, G. Zamora, C. C. Hilgetag, and J. Kurths, Phys. Rev. Lett. **97**, 238103 (2006).
[50] G. Buzsaki *et al.*, Trends Neurosci. **27**, 186 (2004).